Coexistence of Antiferromagnetic and Spin Cluster Glass Order in the Magnetoelectric Relaxor Multiferroic $PbFe_{0.5}Nb_{0.5}O_3$

W. Kleemann,* V. V. Shvartsman,† and P. Borisov‡

Angewandte Physik, Universität Duisburg-Essen, Lotharstrasse 1, D-47048 Duisburg, Germany

A. Kania

Institute of Physics, University of Silesia, PL-40-007 Katowice, Poland

(Received 29 July 2010; published 13 December 2010)

The coexistence of cluster glass with long-range antiferromagnetic order in the relaxor ferroelectric $PbFe_{0.5}Nb_{0.5}O_3$ is elucidated. While the transition at $T_N = 153$ K on the infinite antiferromagnetic cluster induces $3m$ symmetry with large EH^2 magnetoelectric response, the disconnected subspace of isolated Fe^{3+} ions and finite clusters accommodates the cluster glass below $T_g = 10.6$ K with field-induced m' symmetry and EH-type magnetoelectric response. Critical slowing-down, memory and rejuvenation after aging, occurrence of a de Almeida–Thouless phase line, and stretched exponential relaxation of remanence corroborate the glass nature.

DOI: 10.1103/PhysRevLett.105.257202 PACS numbers: 75.85.+t, 75.50.Lk, 77.22.−d, 77.84.Ek

Materials with nanoscale inhomogeneity have attracted increasing interest in modern solid state physics. Quenched disorder is a crucial factor responsible for the coexistence of different ordered states with almost identical free energy. The most spectacular paradigms are found among solid solutions of transition metal oxides, whose phase diagrams are extremely complex [1]. Coupling and controlling different degrees of freedom in such materials opens unprecedented ways to achieve new functionalities. Also in this context, the discussion on the still poorly understood occurrence of *different* thermodynamic phases in one and the same disordered material has been resumed [1].

To address this issue, the most promising candidates are probably homogeneously dilute magnetic compounds, where independent phases may appear due to segregation at the nanoscale. Coexistent spin-glass (SG) and antiferromagnetic (AF) phases were, e.g., proposed in the dilute Ising systems $Fe_{0.55}Mg_{0.45}Cl_2$ and $Fe_{0.6}Mn_{0.4}TiO_3$ [2,3]. This Letter reports on crucial experiments with the disordered AF ferroelectric (FE) compound $PbFe_{0.5}Nb_{0.5}O_3$ (PFN) [4]. On one hand, the chaotic SG ground state has been verified, e.g., via aging experiments below the glass temperature, $T_g \approx 10$ K. Most spectacularly, however, the subspaces accommodating the AF and SG phases are found to possess different effective symmetries, which permit quadratic and linear magnetoelectric (ME) effects, respectively.

The ME effect of PFN is related to its well-known [4] multiferroicity, i.e., the simultaneous occurrence of FE and magnetic ordering [5]. In its $AB\,O_3$ perovskite structure the Fe^{3+} and Nb^{5+} ions randomly occupy the octahedral B sites [6], thus giving rise to two different types of classic disordered states. On one hand, the ionic charge disorder originates quenched electric random fields (RFs) which provoke relaxor ferroelectric behavior [7], which is, however, only weak in PFN [8].

On the other hand, owing to the random occupation of the B sublattice with magnetic Fe^{3+} ions (spin $S = 2$), a dilute antiferromagnet with a Néel temperature $T_N \approx 153$ K is accomplished [9]. Surprisingly, another nonergodic magnetic state appears below $T \approx 10$ K, which has been attributed either to weak ferromagnetism [10] or to a SG state [11–13].

In this Letter we shall give a definite answer in favor of a spin cluster glass (CG) phase, which coexists with AF long-range order as conjectured previously [13]. We argue that both phases are established independently on separate subsystems, as depicted in Fig. 1. The AF state occupies the percolating exchange-coupled Fe^{3+} cluster, while the CG state comprises rare isolated Fe^{3+} ions and unblocked superantiferromagnetic (SAF) Fe^{3+} clusters with uncompensated magnetic moments [14]. In addition to the well-known nonergodicity of the magnetization [11–13], we present new experimental arguments in favor of the CG phase: (i) polydispersive ac susceptibility whose peak position converges at the glass temperature, $T_g \approx 10.6$ K, (ii) memory and rejuvenation after isothermal aging below T_g, and (iii) stretched exponential relaxation of the thermoremanent magnetization after magnetic FC.

Moreover, ME effects prove to be sensitive indicators of the different spin ordering phenomena. We report on the electrobimagnetic ME (β) effect, which reflects the G-type AF spin order on both the percolated and finite-size SAF clusters of Fe^{3+} ions. By contrast, the CG phase reveals an additional bilinear ME (α) effect [10] induced by magnetic FC to below T_g.

The experiments were carried out on a (001)-oriented parallelepiped-shaped sample (volume $V = 3.2 \times 1.6 \times 0.4$ mm^3) cut from a single-phased single crystal of PFN

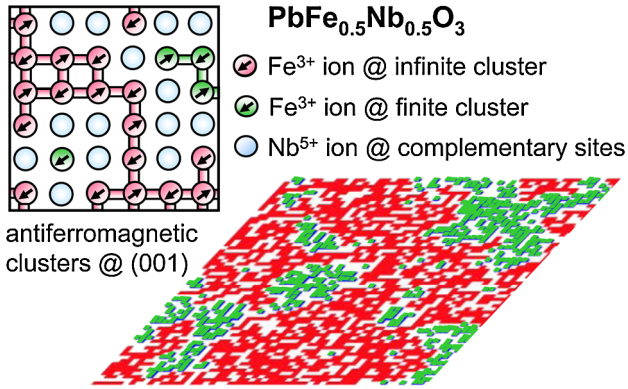

FIG. 1 (color online). Antiferromagnetic Fe^{3+} clusters with projections of ⟨111⟩-oriented spins viewed in (001) cross sections of PFN at different scales.

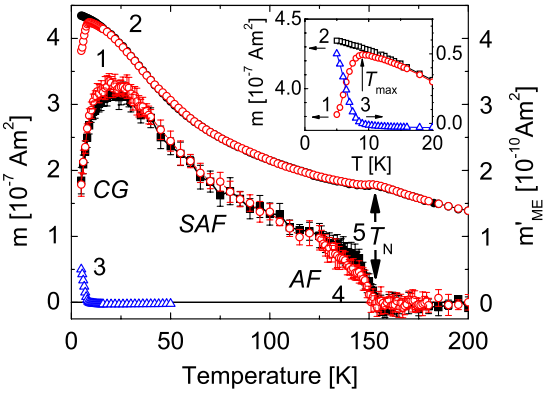

FIG. 2 (color online). Magnetic moment m vs T of PFN(001) obtained on ZFC/FH (curve 1), on FC (curve 2) with $\mu_0 H = 0.1$ T, and on ZFH as TRM (curve 3) (inset: low-T data magnified) (left-hand ordinate). Magnetoelectric moment m'_{ME} vs T obtained with $E_{\mathrm{ac}} = 12.5$ kV/m on ZFC/FH in $\mu_0 H_{\mathrm{dc}} = 0.2$ T and $E_{\mathrm{dc}} = 0$ (curve 4, open circles) or 50 kV/m (curve 5, solid squares) (right-hand ordinate). T_N and the dominance of the AF, SAF, and CG "phases" are indicated.

[15]. Magnetic moments m and ac susceptibility χ' at frequencies $10^{-1} \leq f \leq 10^3$ Hz were measured with a quantum design MPMS-5S superconducting quantum interference device (SQUID). Electric field-induced components of the magnetization, $\boldsymbol{M} = \boldsymbol{m}/V$,

$$\begin{aligned}\mu_0 M_i &= -\partial F/\partial H_i \\ &= \mu_0 \mu_{ij} H_j + \alpha_{ij} E_j + \beta_{ijk} E_j H_k \\ &\quad + \frac{\gamma_{ijk}}{2} E_j E_k + \delta_{ijkl} H_j E_k E_l, \end{aligned} \tag{1}$$

related to the ME Landau free energy expansion [16] are measured using an adapted SQUID susceptometry [17]. It involves external electric and magnetic ac and dc fields along the cubic [001] direction, $E = E_{\mathrm{ac}} \cos\omega t + E_{\mathrm{dc}}$ and H_{dc}, and records the first harmonic ac magnetic moment, $m_{\mathrm{ME}}(t) = (m'_{\mathrm{ME}} - i m''_{\mathrm{ME}}) \cos\omega t$, where

$$\begin{aligned} m'_{\mathrm{ME}} = (&\alpha_{33} E_{\mathrm{ac}} + \beta_{333} E_{\mathrm{ac}} H_{\mathrm{dc}} + \gamma_{333} E_{\mathrm{ac}} E_{\mathrm{dc}} \\ &+ 2\delta_{3333} E_{\mathrm{ac}} E_{\mathrm{dc}} H_{\mathrm{dc}})(V/\mu_o), \end{aligned} \tag{2}$$

and $m''_{\mathrm{ME}} \approx 0$ at $f = \omega/2\pi = 1$ Hz.

Figure 2 shows the magnetic moment m vs T of PFN (001) obtained after zero-field cooling (ZFC) on field heating (FH) with $\mu_0 H = 0.1$ T (curve 1), on subsequent FC from $T = 200$ K to 5 K in the same field (curve 2), and the thermoremanent magnetization, TRM (curve 3), on zero-field heating (ZFH). The well-known AF anomaly [9,10,15] at $T_N \approx 153$ K is virtually independent of the field treatment, while signatures of nonergodicity [10–12,15] are clearly observed at low T (cf. inset to Fig. 2), where the ZFC/FH curve shows a kink at ≈ 10 K, the FC data saturate upon cooling, and the TRM gently falls to zero at ≈ 10 K.

In order to settle the spin-glass conjecture [11–13] we measured the ac susceptibility at a field amplitude $\mu_0 H_{\mathrm{ac}} = 0.4$ mT and frequencies $0.1 \leq f \leq 10^3$ Hz, as shown by the real part χ' vs T in Fig. 3(a). The rounded signal gently shifts to higher temperatures as f increases, and decreases in amplitude. The peak temperature T_m obeys a power law, $f(T_m) \propto (T_m/T_g - 1)^{z\nu}$ [Fig. 3(b)], which is typical of glassy critical behavior [18]. Best fits yield the glass temperature $T_g = 10.6 \pm 1.3$ K [arrow in Fig. 3(a)], and the dynamical critical exponent, $z\nu = 9.0 \pm 2.5$, which compares well with those of canonical and super-SG systems [15]. Obviously the spin dynamics becomes frozen on a glassy backbone below T_g, where the longest relaxation time $\tau_{\max} = (2\pi f)^{-1} \to \infty$. Similar, albeit systematically larger, values of T_g were reported previously (27.6 K [11], 28 ± 2 K [12], ≈ 20 K [13]), while it roughly equals the "critical temperature" $T_c \approx 9.5$ K of the field-induced remanent magnetization [10].

A crucial test of the CG phase rests upon isothermal aging at wait temperatures $T_w < T_g$. Figure 3(c) shows a deep and sharply bounded "hole" burnt at $T_w \approx 7$ K into the difference curve $\Delta m^{\mathrm{ZFC}}(T) = m^{\mathrm{ZFC}}_{\mathrm{wait}}(T) - m^{\mathrm{ZFC}}_{\mathrm{ref}}(T)$ of data recorded on FH in $\mu_0 H = 0.1$ T after ZFC with and without an intermittent stop (wait time $t_w = 10^4$ s at $T_w = 7$ K). The occurrence of the "hole" at T_w (within errors) evidences memory and rejuvenation like in atomic and super SG [18,23], owing to their chaotic ground state properties [19].

Another test examines the shift of the glass temperature in an applied magnetic field along the de Almeida–Thouless–type phase boundary [20],

$$\mu_0 H(T_{\mathrm{AT}}) = A[1 - T_{\mathrm{AT}}(H)/T_{\mathrm{AT}}(0)]^{\alpha}, \tag{3}$$

where $T_{\mathrm{AT}}(0) \equiv T_g$. Anticipating the critical exponent expected for low fields [20], $\alpha = 3/2$, we have plotted the peak temperature $T_{\max}(H)$ of the ZFC-FH magnetization curve (arrow in Fig. 2, inset) vs $(\mu_0 H)^{2/3}$ in Fig. 3(d). The observed linearity for $\mu_0 H \leq 1$ T satisfactorily meets this expectation.

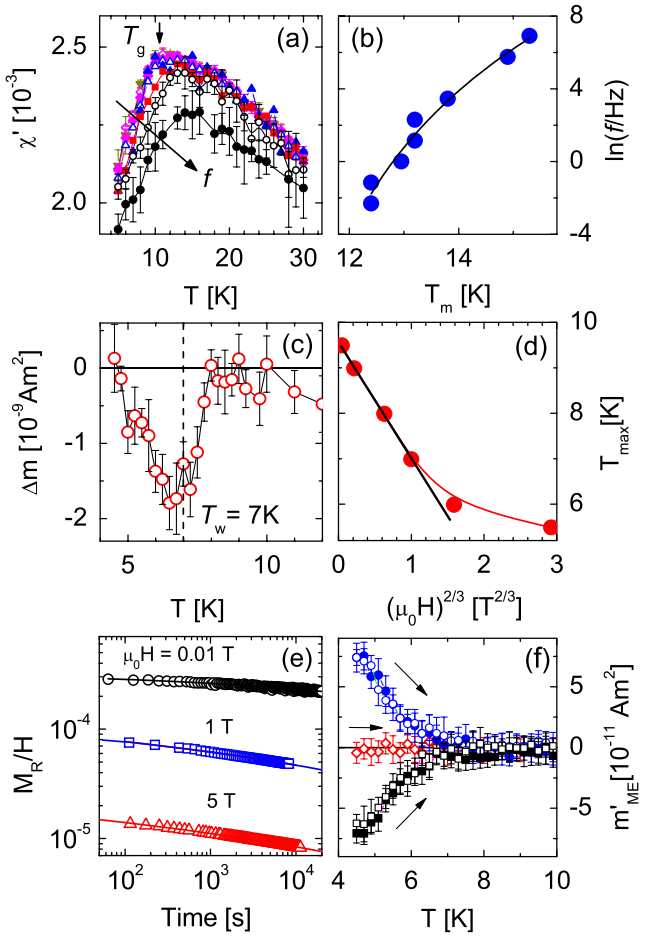

FIG. 3 (color online). (a) ac susceptibility χ' vs T measured with $\mu_0 H_{ac} = 0.4$ mT at frequencies $f = 0.01$, 0.031, 0.1, 0.316, 1, 3.16, 10, 31.6, 100, 316, and 1000 Hz. (b) f dependence of the peak temperature (T_m) of χ' (T) taken from (a), plotted as $\ln(f/\mathrm{Hz})$ vs T_m, and fitted by a critical power law (solid line). (c) $\Delta m = m_{\mathrm{wait}}^{\mathrm{ZFC}} - m_{\mathrm{ref}}^{\mathrm{ZFC}}$ vs T obtained on FH in $\mu_0 H = 0.1$ T after ZFC from $T = 200$ to 4.5 K and waiting for $\Delta t = 10^4$ and 0 s, respectively, at $T_w = 7$ K. (d) de Almeida–Thouless phase boundary approximated by $T_{\max}(H)$ (see arrow in Fig. 2, inset) vs $(\mu_0 H)^{2/3}$ after ZFC to 4.5 K. (e) Relaxation of M_R/H vs t at $T = 5$ K after FC in $\mu_0 H_{dc} = 0.01$, 1, and 5 T, best-fitted to stretched exponentials, Eq. (4). (f) ME moment, m'_{ME} vs T, obtained with $E_{ac} = 25$ kV/m after FC from $T = 160$ to 4.5 K on FH in $\mu_0 H_{dc} = +2$ (upper curve), 0 (middle curve), and -2 T (lower curve), and $E_{dc} = 0$ (solid curve) and 100 kV/m (open symbols).

Typical nonequilibrium dynamics of the CG is shown in Fig. 3(e), where the normalized TRM, M_R/H vs time t, encounters stretched exponential decay,

$$m_{\mathrm{TRM}} = m_0 \exp[-(t/\tau)^{\beta}], \tag{4}$$

after FC in $\mu_0 H = 10$ mT, 1 T, and 5 T, respectively, from $T = 200$ to 5 K at a rate $dT/dt = 10^{-2}$ K/s. This behavior is typical of the isothermal approach to the glassy ground state [21]. Very small exponents, $\beta = 0.16$, 0.11, and 0.09, respectively [cf. best-fitted solid lines in Fig. 3(e)], indicate thermal activation over extremely broad spectra of barrier heights [22].

Finally, the ME response of the sample has been inspected. Figure 3(f) shows the ac moment, m'_{ME} vs T, obtained on ZFH with $E_{ac} = 25$ kV/m after FC from $T = 250$ to 4.5 K in $\mu_0 H = +2$ (upper curve), 0 (middle curve), and -2 T (lower curve), and $E = 0$ (solid curve) and 100 kV/m (open symbols). The ME signal is proportional to the sign and magnitude of $\mu_0 H$, where $m'_{ME}(4.5\ \mathrm{K}) \approx \pm 7.5 \times 10^{-11}$ A m^2 for $\mu_0 H = \pm 2$ T and $\lim_{T \to T_g} m'_{ME} = 0$.

Obviously a *linear* ME (α or EH) effect is encountered, which is conditioned by magnetic FC, but does not explicitly necessitate electric FC. Equation (2) yields the coupling constant (in cubic axis notation) $\alpha_{33}(4.5\ \mathrm{K}) = \mu_0 m'_{ME}/E_{ac} V \approx 1.9 \times 10^{-12}$ s/m in agreement with the results of Watanabe and Kohn [10]. Obviously, the slowly relaxing CG remanence M_R [Fig. 3(e)], together with the ferroelectric state of the underlying PFN lattice (once poled at an early stage of the experiments), provides the correct symmetry frame for the linear ME effect observed. The global CG symmetry corresponds to the monoclinic class m' [10], whose mirror plane with time inversion is defined by both the polar axis and the induced magnetization. Since the temporal relaxation of M_R becomes accelerated upon approaching T_g and data collection was sufficiently slow ($\Delta t \approx 1$ h between 4.5 K and T_g), m'_{ME} vs T decays concavely as $T \to T_g$, unlike the order parameter-like vanishing remanence, σ_0 vs T ("spontaneous" magnetization [10]).

Above T_g a quadratic paramagnetoelectric (β or EH^2) effect remains under $\mu_0 H_{dc} \neq 0$, as shown in Fig. 2 (curve 4), where m'_{ME} is excited after ZFC on FH in $\mu_0 H_{dc} = 0.2$ T by $E_{ac} = 12.5$ kV/m and virtually vanishes above $T_N \approx 153$ K. Below T_N it first behaves order parameter-like down to ≈ 120 K, then gently bends up and attains a peak value, $m'^{\max}_{ME} \approx 3.3 \times 10^{-10}$ A m^2, at $T \approx 18$ K. A steep drop by about 50% follows below $T \approx 15$ K. The coupling constant $\beta_{333}(18\ \mathrm{K}) \approx 1.0 \times 10^{-16}$ s/A [cf. Eq. (2)] is comparable to $\beta_{333}(15\ \mathrm{K}) \approx 1 \times 10^{-17}$ s/A reported previously [23].

An additional static electric field, $E_{dc} = 50$ kV/m, has a minor influence on the ME signal (curve 5). Only close to $T_N (\approx 140$ K) an additional magnetocapacitive (δ or E^2H^2) effect [17] yields a sizable change of $\Delta m'_{ME} \approx 3 \times 10^{-11}$ A m^2. It corresponds to a coupling constant $\delta_{3333} \approx 2.2 \times 10^{-22}$ s m/V A. Most likely, it reflects the spin fluctuations close to the AF transition via spin-pair correlation functions $\langle \mathbf{S}_i \cdot \mathbf{S}_j \rangle$, which enter $\Delta m'_{ME} \approx \delta_{ijkl} \langle \mathbf{S}_i \cdot \mathbf{S}_j \rangle \langle \boldsymbol{\sigma}_k \cdot \boldsymbol{\sigma}_l \rangle$ [16] at virtually constant pseudospin (= polarization)-pair correlation functions, $\langle \boldsymbol{\sigma}_k \cdot \boldsymbol{\sigma}_l \rangle \propto P_s^2$.

The peculiar T dependence of the β effect calls for an extra explanation. Following the mean field calculation for G-type AF ordered $EuTiO_3$ [24], we expect

$$\chi^{me}_{333} = \partial \langle S^z \rangle / \partial E_z = 24 \beta \chi_m^2 \chi_e E H^2, \tag{5}$$

where the prefactor 24 accounts for the 50% dilution of the magnetic B site sublattice. The only contribution with noticeable T dependence below T_N is the AF susceptibility χ_m, which is shown in Fig. 2 (curves 1 and 2) and qualitatively resembles χ^{me}_{333} except for $T \lesssim T_N$ and $T > T_N$.

At temperatures $T_N < T < T_{c2} = 355$ K, χ^{me}_{333} seems to vanish within errors, although the monoclinic space group of PFN, Cm [8], permits all but one diagonal β couplings [25]. Closer inspection reveals very small, virtually constant negative values, e.g. $\beta_{333}(155\ \mathrm{K}) \approx -1.5 \times 10^{-18}$ s/A (not shown). The observed spontaneous ascent to large and positive β values for $T < T_N$ (Fig. 2) thus clearly excludes the persistence of Cm, in disagreement with [8], but rather favors conversion into rhombohedral point group symmetry, $3m$ [23]. Most likely, this is related to the trigonal exchange striction, $s_{111} \propto \langle \mathbf{S}_i \cdot \mathbf{S}_j \rangle$, due to the G-type spin ordering [26], and explains the proportionality of χ^{me}_{333} to the squared AF order parameter, $\boldsymbol{L}^2 \tilde{\propto} \langle \boldsymbol{S}_i \cdot \boldsymbol{S}_j \rangle$, as observed just below T_N (labeled as "AF" in Fig. 2).

In order to understand the monotonic increase of both χ_3 and χ^{me}_{333} below ≈ 140 K, we recall that the AF long-range order is restricted to the percolating spin cluster on the B sublattice. However, in view of Fig. 1 we also have to account for finite-sized SAF clusters, which explain the Curie-type "superparamagnetic" increase of both χ_m (Fig. 2, curves 1 and 2) and $\chi^{me}_{333} \propto \chi^2_m$ (labeled as "SAF" at curves 4 and 5). Only at $T < 25$ K does m'_{ME} start to drop, presumably as a consequence of a proper β effect of the CG, whose precursor tail starts at $\approx 2T_g$ (labeled as "CG" in Fig. 2). Its negative sign emphasizes its independence of the AF phase, where $\beta > 0$.

In view of the large distances between isolated Fe^{3+} ions and SAF clusters (Fig. 1), the global coherence of the CG state appears enigmatic. If only the nearest neighbor superexchange interaction via Fe^{3+}-O^{2-}-Fe^{3+} links were available, the CG would probably have no chance to form at temperatures as high as 10 K. Long-range dipolar coupling via the rare excess SAF moments probably helps stabilize the glassiness. Crucially, however, the classic O^{2-} mediated superexchange along $\langle 001 \rangle$ is enhanced in PFN by the superexchange along $\langle 111 \rangle$ via Pb^{2+} ions [27]. This helps the infinite CG subsystem to coalesce and to reveal genuine glassy properties and an effective m' symmetry, as demonstrated in Figs. 2 and 3.

In conclusion, we have derived a coherent view of the magnetic behavior of the multiferroic relaxor crystal PFN within a cluster approach. Apart from the well-known AF long-range order on a percolating exchange-coupled Fe^{3+} cluster as evidenced, e.g., by sharp elastic neutron Bragg peaks at all temperatures below T_N [13], we observe canonical magnetic glass freezing in an independently "percolating" system of clusters and isolated Fe^{3+} ions. This is at the origin of diffuse neutron scattering and enhanced muon spin rotation in the dynamic freezing range, $T_g < T < 2T_g$ [13]. The different "effective" point group symmetries, $3m$ and m', of the interpenetrating phases AF and CG, respectively, underline their independence. This novel feature of disordered systems merits further research, e.g., on the yet poorly understood "AF spin glasses" $Fe_{0.55}Mg_{0.45}Cl_2$ and $Fe_{0.6}Mn_{0.4}TiO_3$ [2,3], and other correlated transition metal oxides [1].

We thank B. Barbara, Institut Néel, Grenoble, for fruitful discussions; P. Stauche, Ruhr-Universität Bochum, for XRD analyses; DFG (SFB 491) and FNP for financial support.

*To whom all correspondence should be addressed.
wolfgang.kleemann@uni-due.de
†Now at Institut für Materialwissenschaft, Universität Duisburg-Essen, D-45141 Essen, Germany.
‡Now at Department of Chemistry, University of Liverpool, Liverpool L69 7ZD, United Kingdom.

[1] E. Dagotto, Science **309**, 257 (2005).
[2] Po-Zen Wong *et al.*, Phys. Rev. Lett. **55**, 2043 (1985).
[3] H. Yoshizawa, Phys. Rev. Lett. **59**, 2364 (1987).
[4] G. A. Smolenskii *et al.*, Sov. Phys. Tech. Phys. **3**, 1981 (1958).
[5] H. Schmid, Ferroelectrics **162**, 317 (1994).
[6] S. A. Ivanov *et al.*, J. Phys. Condens. Matter **12**, 2393 (2000).
[7] V. Westphal, W. Kleemann, and M. D. Glinchuk, Phys. Rev. Lett. **68**, 847 (1992).
[8] N. Lampis, P. Sciau, and A. Geddo Lehmann, J. Phys. Condens. Matter **11**, 3489 (1999).
[9] V. A. Bokov *et al.*, Sov. Phys. JETP **15**, 447 (1962).
[10] T. Watanabe and K. Kohn, Phase Transit. **15**, 57 (1989).
[11] A. Kumar *et al.*, Appl. Phys. Lett. **93**, 232902 (2008).
[12] A. Falqui *et al.*, J. Phys. Chem. B **109**, 22967 (2005).
[13] G. M. Rotaru *et al.*, Phys. Rev. B **79**, 184430 (2009).
[14] L. Néel, Acad. Sci. Paris C.R. **253**, 9 (1961).
[15] A. Kania, E. Talik, and M. Kruczek, Ferroelectrics **391**, 114 (2009).
[16] V. V. Shvartsman, S. Bedanta, P. Borisov, W. Kleemann *et al.*, Phys. Rev. Lett. **101**, 165704 (2008).
[17] P. Borisov, A. Hochstrat, V. V. Shvartsman, and W. Kleemann, Rev. Sci. Instrum. **78**, 106105 (2007).
[18] P. E. Jönsson, Adv. Chem. Phys. **128**, 191 (2003).
[19] A. J. Bray and M. A. Moore, Phys. Rev. Lett. **58**, 57 (1987).
[20] J. R. L. de Almeida and D. J. Thouless, J. Phys. A **11**, 983 (1978).
[21] R. V. Chamberlin, G. Mozurkewich, and R. Orbach, Phys. Rev. Lett. **52**, 867 (1984).
[22] R. G. Palmer *et al.*, Phys. Rev. Lett. **53**, 958 (1984).
[23] B. Howes *et al.*, Ferroelectrics **54**, 317 (1984).
[24] V. V. Shvartsman, P. Borisov, W. Kleemann, S. Kamba *et al.*, Phys. Rev. B **81**, 064426 (2010).
[25] E. Ascher, Philos. Mag. **17**, 149 (1968).
[26] L. C. Bartel and B. Morosin, Phys. Rev. B **3**, 1039 (1971).
[27] I. P. Raevski *et al.*, Phys. Rev. B **80**, 024108 (2009).